Study on the Method to Measure Thermal Contact Resistance Within Press Pack IGBTs

Erping Deng, *Member, IEEE*, Zhibin Zhao, *Member, IEEE*, Peng Zhang, Xiaochuan Luo, Jinyuan Li, and Yongzhang Huang

***Abstract*—The accurate measurement of the thermal contact resistance between multilayers within press pack insulated gate bipolar transistors (PP IGBTs) is significant for optimizing their thermal resistance to improve reliability, as thermal contact resistance accounts for about 50% of their total thermal resistance under the rated clamping force. The components within PP IGBTs are very small, and an external clamping force is needed to ensure they work normally. Thus, the methods of thermal contact resistance measurement of steady-state and transient methods are no longer suitable. In this paper, the method of thermal structure function is proposed to measure the thermal contact resistance between multilayers within PP IGBTs. The accurate measurement of the transient thermal impedance curve of PP IGBTs is the key to this method, and it can then be transformed to a cumulative and differential structure function to determine the thermal contact resistance accurately. A single fast recovery diode chip submodule is fabricated to predict the thermal contact resistance behavior within PP IGBTs in this experiment, and the experimental results agree well with theoretical values. Furthermore, the influence of both the high temperature and the clamping force on the thermal contact resistance can also be obtained from this method accurately.**

***Index Terms*—Press pack insulated gate bipolar transistors (PP IGBTs), single fast recovery diode (FRD) chip submodule, thermal contact resistance, thermal structure function.**

I. INTRODUCTION

TO MEET the growing requirements of insulated gate bipolar transistor (IGBT) device applications, capacity and reliability have become great challenges for IGBT devices. Press pack IGBTs (PP IGBTs) have gradually been applied to high-voltage and high-power density applications, such as electric locomotives and high-voltage direct current transmission, for their higher reliability, double-side cooling, higher power density, and easy to connect in series [1], compared to typical wire-bonded IGBT modules. A cross-section of the internal structure of the PP IGBT is shown in Fig. 1, where it may be observed that the PP IGBT has a multilayered structure. Two copper electrodes (collector and emitter pole) provide both the electrical and thermal paths for the silicon chips, and the silicon IGBT chips are sandwiched by two molybdenum plates that aid in the uniform distribution of the clamping force. A silver shim plate, together with a silicon IGBT chip and two molybdenum plates, is to form a chip assembly. An external clamping force is required to maintain both the electrical and thermal contact of all components within PP IGBTs through dual heatsinks. Thermal contact resistance existing between multilayers within PP IGBTs is a very important parameter for thermal resistance optimization and reliability improvement, as it accounts for about 50% of the total thermal resistance under the rated clamping force [2].

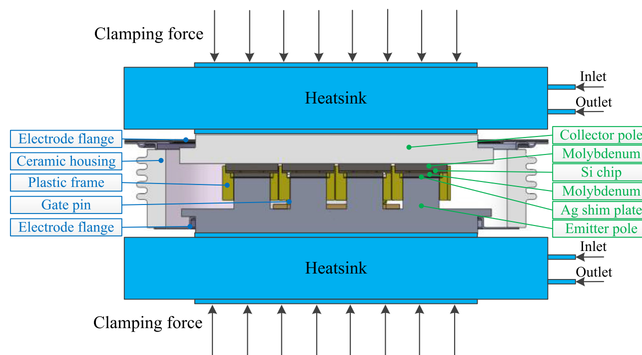

Fig. 1. Cross-sectional schematic diagram for PP IGBTs.

When two rough surfaces contact with each other, actual contact only occurs at several discrete spots or microcontacts, while the noncontacting areas form vacuums or are filled with some medium (such as air, water, oil, etc.). The actual contact area accounts for about 0.01–0.1% of the nominal contact area, and the proportion only increases to 1–2% under a contact pressure of 10 MPa [3]. A relatively small actual contact area and low thermal conductivity of the interfacial gases lead to a large

Manuscript received October 31, 2017; revised March 12, 2018; accepted April 26, 2018. Date of publication April 30, 2018; date of current version December 7, 2018. This work was supported in part by the National Natural Science Foundation of China—State Grid Corporation Joint Fund for Smart Grid under Grant U1766219; and in part by the State Key Laboratory of Alternate Electrical Power System with Renewable Energy Source, North China Electrical Power University under Grant LAPS17003. Recommended for publication by Associate Editor S. S Ang. *(Corresponding authors: Erping Deng; Zhibin Zhao.)*

E. Deng is with the State Key Laboratory of Alternate Electrical Power System with Renewable Energy Sources, North China Electric Power University, Beijing 102206, China, and also with the Global Energy Interconnection Research Institute, State Grid Corporation of China, Beijing 102211, China (e-mail:

See http://www.ieee.org/publications_standards/publications/rights/index.html for more information.

thermal resistance when heat flows across the interface. It is always called thermal contact resistance [4], [5].

This is a complex parameter affected by material properties, surface morphology, contact pressure, temperature, etc. [6], [7]; thus, the precision of a test bench will be a great challenge to the measurement. At present, steady-state and transient methods are used to estimate the thermal contact resistance, and a steady-state method is the most commonly used. The temperature difference between two contact interfaces can be achieved by linear fitting after it has been measured between two samples in the steady-state method [8]. The temperature distribution of the specimen will not only be disturbed by the embedded thermocouple, but the accuracy of the adjacent measured temperature will also be influenced, since this method requires a thermocouple to measure the temperature. Most importantly, many thermocouples must be located in the samples; thus, the steady-state method is not suitable for specimens whose dimensions are as small as a millimeter, just like the components within PP IGBTs. In order to overcome some disadvantages of the thermocouple method, some scholars have proposed an infrared imaging system with an accuracy of 0.1 °C instead of thermocouples to record the temperature of two-dimensional interfaces. The accuracy is improved significantly, but an error of about 23% still remains [9]. An optical–thermal method is widely used among the transient thermal contact resistance measurement methods [10], [11]. It can be obtained by the phase difference of heat wave and modulation wave after encountering the interfaces. However, the accuracy of the optical–thermal method is affected by the interface characteristics, as the heat wave is diffused at the contact interface, destroying their phase relationship [12].

All the methods mentioned above are for the thermal contact resistance measurement between power semiconductor devices and heatsinks, or among copper busbar junctions. That is, they are for measuring the thermal contact resistance outside power semiconductors rather than within them. Furthermore, the components within PP IGBTs are too small and encapsulated, let alone the accuracy of those methods is not enough. Therefore, the accuracy measurement of the thermal contact resistance within PP IGBTs becomes a big problem because no existing method is able to measure it.

For the measurement of thermal contact resistance within PP IGBTs, Poller *et al*. [13] have calculated it through an iterative algorithm of a multi-object genetic algorithm based on the combination of experiments and finite element methods. At each iteration, the match between the finite element solution and the experimental setup is verified by comparing some predefined target parameters calculated by the finite element model with the actual measurements. However, the thermal contact conductivity of the interfaces between the same combinations of material is assumed to be the same to reduce complexity. Thus, the accuracy of this method is limited because the thermal contact resistance of the same combination of material is different caused by the different surface roughness [14]. And furthermore, the deviation of the thermocouple still exists. Deng *et al*. [14] proposed an indirect method to measure the change of the junction-to-case thermal resistance to predict the change of thermal contact resistance with the assumption that the bulk thermal resistance of a specific material layer is not sensitive to the clamping force or temperature. Furthermore, with the experimental results of the nanosilver sintered one, the thermal contact resistance and its deviation with the clamping force and temperature can be obtained. However, the procedure of this experiment is relatively complex and these two methods mentioned are the indirect method to get the thermal contact resistance. Thus, a direct and simple method to measure the thermal contact resistance within PP IGBT should be proposed.

The direct measurement of thermal contact resistance within PP IGBTs is still impossible with the limits that no probes can be placed between two test samples and the needed clamping force system. Furthermore, the optical–thermal or other noncontact methods, for example, thermal camera method [15], are not suitable for PP IGBTs because the chips are clamped and encapsulated. Therefore, the method of thermal structure functions is proposed in this paper to measure the thermal contact resistance between multilayers within PP IGBTs directly, and the experimental results agree well with theoretical values. Furthermore, the influence of high temperature and the clamping force on the thermal contact resistance can also be obtained accurately through this method. This also presents the validity and advancement of the proposed method. Meanwhile, the experimental results are also compared with the results from the indirect method.

The structure of this paper is as follows. We present the internal structure of PP IGBTs and the status of methods of thermal contact resistance measurement in the introduction. The basic principle of thermal structure functions and the determination of thermal contact resistance based on structure functions are introduced in Section II. In Section III, a single fast recovery diode (FRD) chip (3300 V/100 A) submodule is fabricated to predict the thermal contact resistance behavior within PP IGBTs, and the experimental results are verified by the theoretical values. The conclusions based on the experimental results are shown in Section IV.

II. Principle of Measurement

Thermal contact resistance within PP IGBTs can be directly determined by cumulative and differential structure functions, and these are derived from a transient thermal impedance curve. Thus, the key to this method is to measure the transient thermal impedance curve of the studied PP IGBTs accurately.

A. Transient Thermal Impedance Curve

Fig. 2 shows the principle of the transient thermal impedance curve measurement [16]. Two direct current sources provide the heating and sensing currents for the device under test (DUT). A heating current $I_{\rm drive}$ is flowed into the DUT to heat it to thermal equilibrium, and then the heating current $I_{\rm drive}$ is switched to a sense current $I_{\rm sense}$ to measure the voltage drop during the cooling phase. The junction temperature T_j during the cooling phase is acquired through the recorded voltage drop and K factor, which is the relationship between voltage drop and junction temperature for short [17]. Finally, the thermal impedance

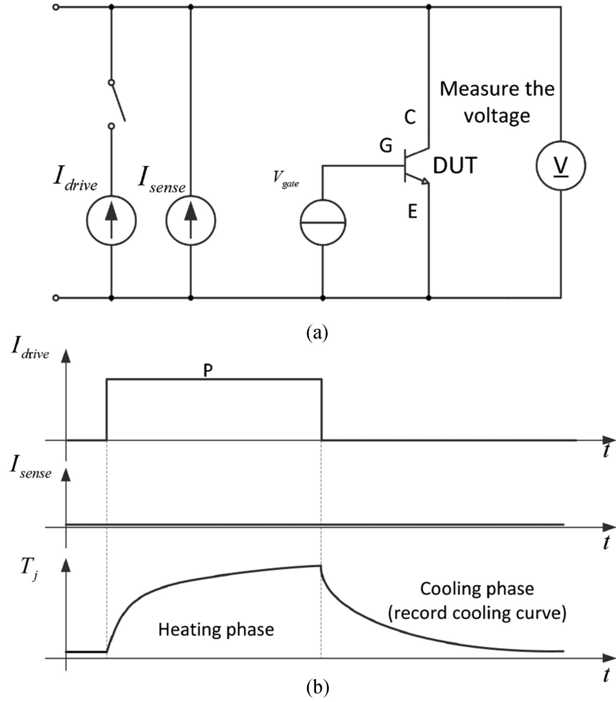

Fig. 2. Principle diagram of the transient thermal impedance curve measurement. (a) Test circuit. (b) Thermal transient test sequence.

$Z_{\text{th,cooling}}(t)$ of the DUT during the cooling phase can be obtained by (1) [18]. Furthermore, the junction behavior of the heating phase is similar to the cooling phase, so the thermal impedance $Z_{\text{th,heating}}(t)$ during the heating phase can be calculated by (2) [19] as follows:

$$Z_{\text{th,cooling}}(t) = \frac{T_j(t) - T_j(t=0)}{P} \tag{1}$$

$$Z_{\text{th,heating}}(t) = Z_{\text{th,cooling}}(t=0) - Z_{\text{th,cooling}}(t). \tag{2}$$

B. Structure Functions

As stated before, the thermal impedance needs a reference temperature that will not change during the test that $T_j(t = 0)$ can be used as the reference temperature. Actually, the case temperature of the DUT will be changed during the measurement (usually will increase) and this value is not suitable for the reference temperature. The heatsink or the inlet or outlet temperature or the average value of the inlet and outlet temperature of the cooling system will not change so much that this value is also used as the reference temperature. And furthermore, in this paper, we mainly considered the thermal resistance or thermal contact resistance within PP IGBTs. Thus, the transient thermal impedance is from junction to heatsink and describes the thermal resistance change from the junction to the case during the heating/cooling phase of power semiconductors, and includes some important thermal information for each specific material layer within the DUT. Cumulative and differential structure functions can be derived from it through mathematical transformation, for example, deconvolution and discretization. The structure functions to determine the thermal contact resistance between interfaces are shown in Fig. 3.

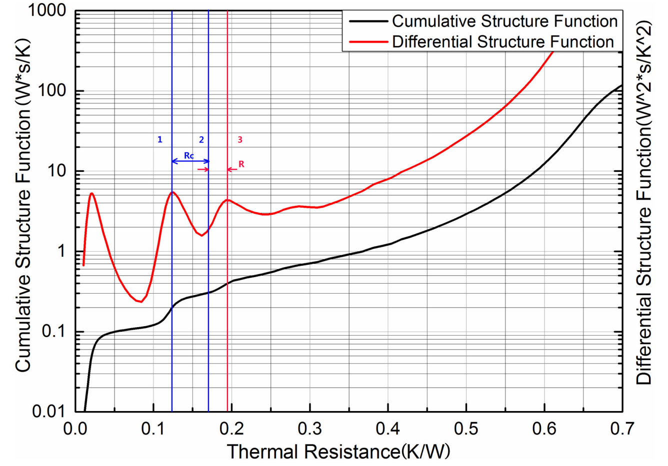

Fig. 3. Cumulative and differential structure functions to determine the thermal resistance and thermal contact resistance.

The cumulative and differential structure function formulas are shown in the following equations, respectively, where $C(R)$ is the cumulative structure function (W∗s/K), $\rho(R)$ denotes the differential structure function (W^2∗s/K^2), R represents the thermal resistance (K/W), A is the sectional area (m^2), k is the thermal conductivity (W/(m∗K)), c is the constant-pressure specific heat (J/(kg∗K)), and ρ is the material density (kg/m^3):

$$C(R) = c \cdot \rho \cdot k \cdot A^2 \cdot R \tag{3}$$

$$\rho(R) = \frac{dC(R)}{dR} = c \cdot \rho \cdot k \cdot A^2. \tag{4}$$

Cumulative structure function denotes the relationship between the thermal resistance and thermal capacity of the heat path from the junction to heatsink, and the junction is always the origin of those structure functions. Any changes in the section area of the specific material layer or of the heat flux flows into the different material layers will lead to slope change in the cumulative structure function. That is to say that each specific material layer has a special slope and this can help us to determine the bulk thermal resistance of each specific material layer. Furthermore, the contact interface has a much smaller slope due to the bad thermal conductivity and small specific heat of the air in the gap. The differential structure function is the gradient of the cumulative structure function of the thermal resistance. At the same locations, any changes in the slope of cumulative structure function will lead to a peak point in the differential structure function. From the differential structure function, it can be seen that the peak point corresponds to the interface between two specific materials. Thus, the thermal resistance between blue line 1 and red line 3 is the sum of R and R_c. As shown in (3), specific material with the same cross-section corresponds to the same slope of the cumulative structure function. Thus, the value R_c between blue line 1 and blue line 2 is the thermal contact resistance with a smaller slope, and the value R between blue line 2 and red line 3 is the bulk thermal resistance. And it is quite easy to recognize each layer according to their structure.

III. Experiments

A. Test Bench

The fixture of the commercial thermal resistance tester is not suitable for PP IGBTs because of their special packaging style and working conditions. For this paper, we designed two fixtures for PP IGBTs, and the thermal transient tester (*T3Ster*) is used to measure the transient thermal impedance curve of the studied PP IGBTs as a higher time resolution is needed in this measurement to record the transient response.

According to the principle of transient thermal impedance measurement, a K factor [17], which accounts for the relationship between junction temperature and voltage drop, should be measured for the junction temperature estimation during the test, and then the transient thermal impedance is recorded. The fixtures for the K factor and transient thermal impedance curve measurement are shown in Fig. 4.

A total of four bolt nuts are used to constrain the displacement in order to sustain the desired clamping force, which is given by a standard pressure machine. A disc spring is needed to compensate the physical movements during the process of clamping and thermal expansion. The clamping force has an extremely slight influence on the K factor as long as the studied PP IGBT is contacted well, because the measurement current is very small [13]. Fig. 5 shows the results of the 3300 V/360 A PP IGBT manufactured by Westcode under 5 and 8 kN with a constant sense current of 20 mA. The results show that the fixture can fully satisfy the measurement requirements because the slopes (°C/V) are almost identical, except for a difference of 0.02 (°C) in the intercept.

The fixture to measure the transient thermal impedance curve consists of heatsinks, a DUT, a disc spring, a clamping force sustaining plate, a hydraulic pump, and a pressure sensor. Dual heatsinks are used to supply the needed clamping force and heat dissipation path. This fixture can easily realize the cathode/anode-side and double-side cooling for the DUT via managing the dual heatsinks. An epoxy resin plate with low thermal conductivity and high compressive modulus can be inserted into the interface between the heatsink and the case surface to realize the thermal adiabatic when we need one-side cooling with other side adiabatic during the test. The clamping force uniformity on the surface is also very important for the results. Thus, a hemisphere is proposed in this fixture because it can be used for the surface flatness adjustment. As mentioned above, the disc spring is needed to compensate the physical movements during the process of clamping and thermal expansion. The clamping force sensor, which is mechanically connected in series with the DUT, is used to record the clamping force of the DUT and to display in real-time. The hydraulic pump provided a continuously adjustable clamping force ranges up to 50 kN, which fully satisfied the requirements of all ratings of PP IGBTs.

B. Object of Experiment

In the high-voltage and high-power-density application, multiple silicon chips are connected in parallel in PP IGBTs to increase the current rating to meet the application requirements; therefore, some differences inevitably exist among these chips, especially the current [20], clamping force [21], and temperature distribution [22]. Meanwhile, the relationship of the thermal contact resistance among multichips is also in parallel because multichips in PP IGBTs are connected in parallel. Actually, the internal environment of PP IGBTs is very complex and the electrical, thermal, and mechanical physics fields are coupled with each other. For example, the collector current and junction temperature distribution are influenced by the clamping force distribution within PP IGBTs through the electrical and thermal contact resistance [23], [24]. The clamping force distribution is also greatly affected by high temperature, the tolerances between

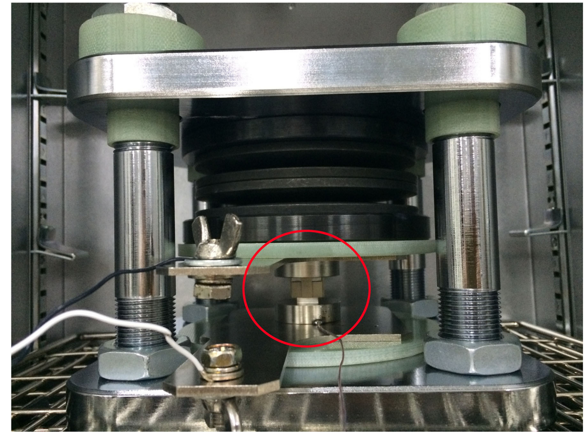

(a)

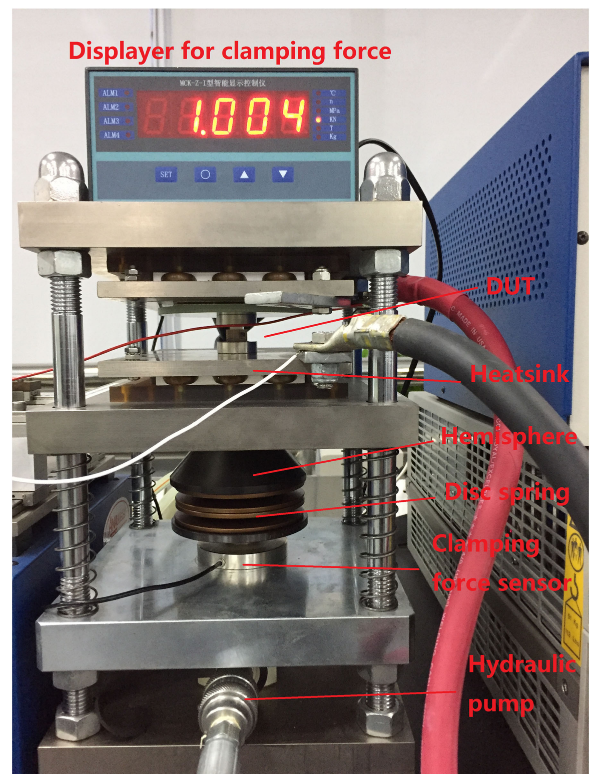

(b)

Fig. 4. Measurement fixtures for PP IGBTs. (a) K factor measurement fixture. (b) Transient thermal impedance measurement fixture.

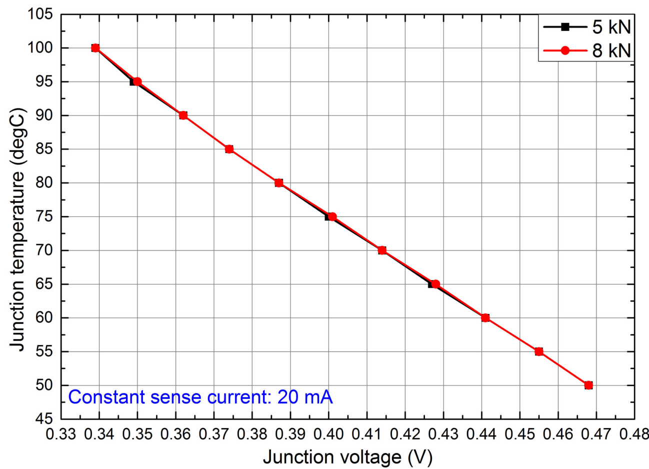

Fig. 5. Comparison between voltage–temperature calibration curves (*K* factor) measured with a clamping force of 5 and 8 kN.

the assembled silicon chip, and so on [25]–[28]. Furthermore, the thermal contact resistance is also significantly influenced by the clamping force and temperature within PP IGBTs [14], and the difference in the clamping force and temperature among those chips also leads to some distinction in the thermal contact resistance. We can see that the thermal contact resistance within PP IGBTs is very complex and affected by many factors caused by multiparalleled chips. Thus, the thermal contact resistance of each layer cannot be clearly revealed through the thermal contact resistance of PP IGBTs.

In order to exclude interference factors from multiparalleled chips, a single FRD chip submodule is fabricated in this paper to predict the thermal contact resistance behavior within PP IGBTs. The structure diagram is shown in Fig. 6, and the object in the test bench is also marked in red in Fig. 4. Two copper electrodes (cathode and anode pole), an FRD chip, two molybdenum plates surrounding the FRD chip, and a silver shim plate form a single FRD chip submodule. The reason why we used a single FRD chip rather than a single IGBT chip submodule is to reduce the experiment complexity, because an external constant voltage is required to apply to the IGBT chip's gate so the device channel is open and the current flows through during the measurement. Meanwhile, grooves are needed to shape into the pedestals, as well as other components on the emitter side, for the gate pin of the housing. Furthermore, the thermal contact resistance behavior rather than the absolute value of the single FRD chip submodule, such as the change trend with the clamping force and high temperature, is the same as the single IGBT chip submodule. This is because the single FRD chip assembly within PP IGBTs has the same packaging structure and other components with the IGBT chip. Thus, the single FRD chip submodule is accurate enough for the prediction of the thermal contact resistance behavior within PP IGBTs. Meanwhile, the measurement of the thermal contact resistance of the FRD chip submodule is the foundation for the single IGBT chip submodule and multichips paralleled PP IGBTs. It is also very meaningful for the optimization of thermal resistance to improve the reliability and the analysis on the collector current, junction temperature, and clamping force distribution within PP IGBTs.

The equivalent Cauer thermal network of the single FRD chip submodule is shown in Fig. 6(c). *F* is the contact clamping force, *P* is the power dissipation of the FRD chip, T_j is the junction temperature, T_{c_c} is the case temperature of the cathode side, and T_{c_a} is the case temperature of the anode side. The letters *a* and *b* denote the distance from the PN junction to the surface of the cathode and anode, respectively. R_x and C_x represent the thermal resistance and capacity of each specific material layer. R_{c_x} and C_{c_x} denote the thermal contact resistance and capacity of the contact interface. The cooling system outside the case surface is defined as the cold plate. It is well known that junction temperature represents the maximum temperature in junction and the PN junction or the heat source is defined as the origin of the thermal network. Thus, the bulk thermal resistance of the whole FRD chip can be divided into two parts and *a* is much bigger than *b* as the PN junction is much closer to the anode surface, especially for high voltage chips.

The network of the submodule has two paralleled heat paths while it is double-side cooling and each heat path has bulk thermal resistance of specific material layer and thermal contact resistance of the contact interface. Thereby, the thermal resistance/thermal contact resistance of the submodule with double-side cooling is the parallel relationship of the value with cathode-side cooling ($R_{jc(c)}$) and anode-side cooling ($R_{jc(a)}$). It is very difficult to distinguish the actual thermal contact resistance of each contact interface with this paralleled relationship. Furthermore, the thermal heat flow from the junction to the cathode and anode side of the housing is asymmetric as their structure is different. It is impossible to control the case surface or heatsink temperature of the cathode and anode sides to be the same as the reference temperature when the submodule is double-side cooling. In this paper, the transient thermal impedance with the cathode-side cooling is, therefore, measured with the anode-side adiabatic to predict the thermal contact resistance within the single FRD chip submodule. A thickness of 2 mm epoxy resin plate with low thermal conductivity and high compressive modulus is inserted into the interface between the anode surface and heatsink to realize the thermal adiabatic condition. Furthermore, the heatsink of the anode side is not working.

C. Experimental Results

According to the mounting instruction from the PP IGBTs manufactures such as ABB [29] and Westcode [30], a clamping pressure of approximately 1.2 kN/cm^2 is ideal for PP IGBTs. Therefore, a clamping force of 1 kN is applied to the submodule according to its clamped area and the aforementioned standard pressure. The transient thermal impedance curve of the cathode-side cooling under the rated clamping force (@1 kN) is measured, and the cumulative and differential structure functions are derived and shown in Fig. 7. The horizontal axis denotes the sum of thermal resistance along with the heat flow path of the single FRD chip submodule from the junction to heatsink and the junction is always the origin. Along with the direction of the thermal resistance increase, the data on the horizontal axis should be

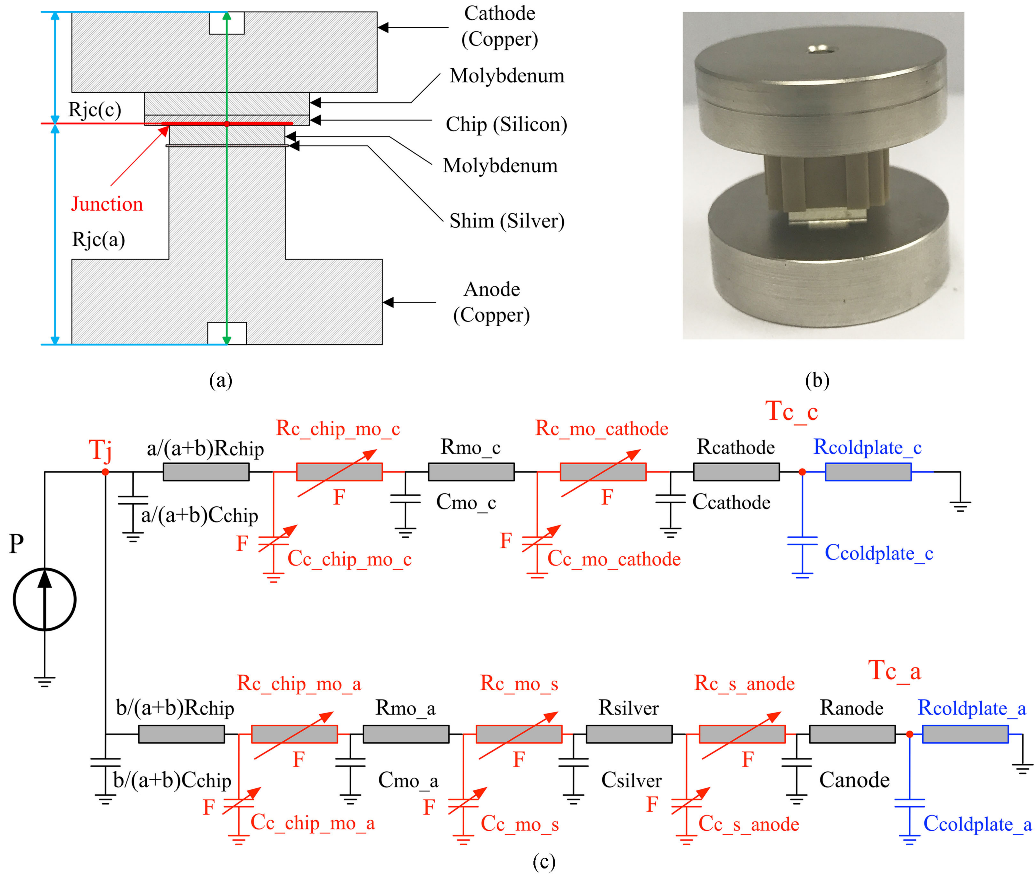

Fig. 6. Single FRD chip submodule for transient thermal impedance curve measurement. (a) Schematic diagram of the single FRD chip submodule. (b) Submodule under test. (c) Equivalent Cauer thermal network of the submodule.

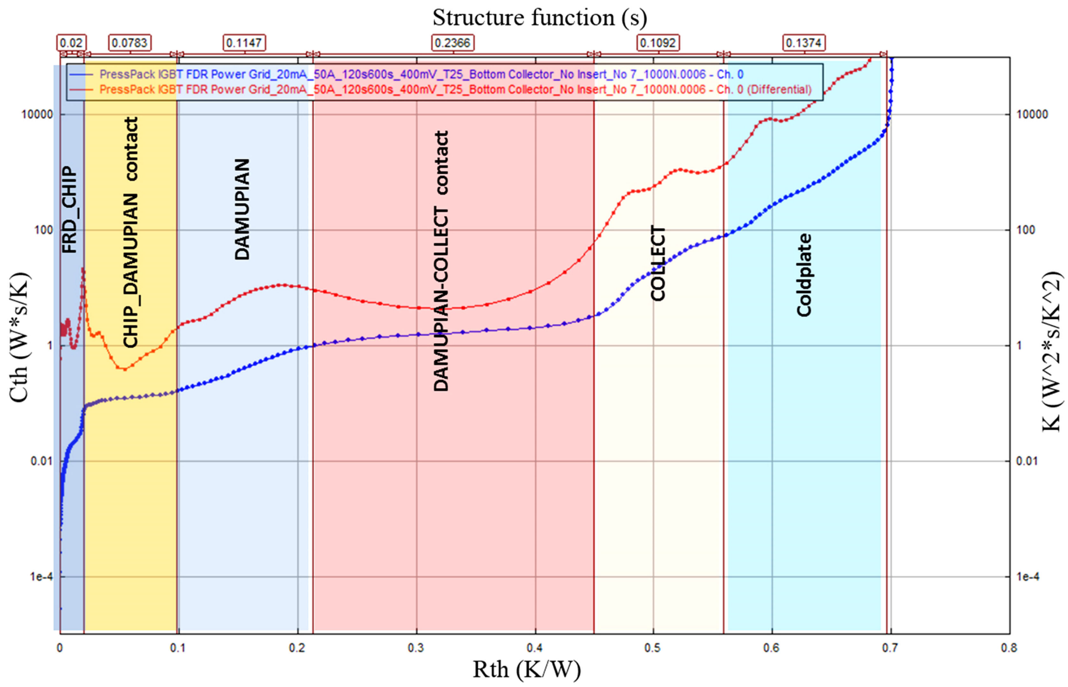

Fig. 7. Cumulative and differential structure functions for the determination of thermal contact resistance.

in the following sequence: "the bulk thermal resistance of the FRD chip," "thermal contact resistance of the contact interface between the silicon chip and molybdenum plate," "molybdenum plate thermal resistance," "thermal contact resistance between molybdenum plate and the cathode pole," "cathode pole thermal resistance," and "other external thermal resistance" (short for cold-plate thermal resistance) according to the packaging structure of the single FRD chip assembly.

And then to determine the exact value of thermal resistance and thermal contact resistance, as stated before, in the cumulative structure function, each specific material layer has a different slope and this helps to identify each material layer. In most practical situations, the gap thickness between two contacting bodies is quite small (<10 μm), and the microcontact gaps are always air-filled. The thermal conductivity and heat capacity of air are relatively low, so the thermal contact resistance is relatively large and the thermal contact capacity is relatively small. Therefore, the contact interface corresponds to the area of the cumulative structure function with a slight change of thermal capacity and a large change of thermal resistance. That is to say, it corresponds to a very small slope in the cumulative structure function. The specific material layer presents a large slope in the cumulative structure function. As shown in Fig. 7, there are two thermal contact resistances existing in the cathode side of the FRD chip assembly with two small slope areas in the structure function. And the thermal contact resistance corresponding to areas 1 and 2 is that between the FRD chip and molybdenum in the case of area 1, and between molybdenum and the cathode for area 2. The experimental results show that the total thermal contact resistance of these two interfaces is 0.3149 K/W and accounts for about 56.3% of the total thermal resistance (0.5588 K/W) under the rated clamping force of 1 kN.

The dimensions of the 3300 V/100 A FRD chip studied in this paper are 13.53 mm × 13.53 mm × 0.41 mm, and its measured thermal conductivity is 117.5 W/(m∗K), so the theoretical thermal resistance of the FRD chip is about 0.019 K/W. The PN junction of this FRD chip is about 10 μm (P+ area couples with the metallization layer) under the anode surface and it is much smaller than the thickness of 410 μm. From the thermal network shown in Fig. 6(c), we can see that a is much bigger than b and the thermal resistance of the FRD chip in the cathode side is almost the value of the whole FRD chip of 0.019 K/W. It conforms to good accuracy to the measured thermal resistance of 0.02 K/W, as shown in Fig. 7. Furthermore, the above-mentioned results indicate that both the bulk thermal resistance of specific material layers and the thermal contact resistance between specific layers can be clearly identified.

The thermal contact resistance between multilayers within the single FRD chip submodule is not only associated with the material characteristics and surface morphology but is also affected by the high temperature and clamping force [14]. In this paper, the influence of the high temperature and the clamping force on the thermal contact resistance of the single FRD chip submodule is also measured through this thermal structure function method. The thermal contact resistance can be directly reflected on the thermal structure functions when it changed with the temperature and clamping force. So, we can know exactly which part is the bulk thermal resistance and which part is the thermal contact resistance. Therefore, according to the influence, the thermal contact resistance and bulk thermal resistance can be better discriminated through the structure functions.

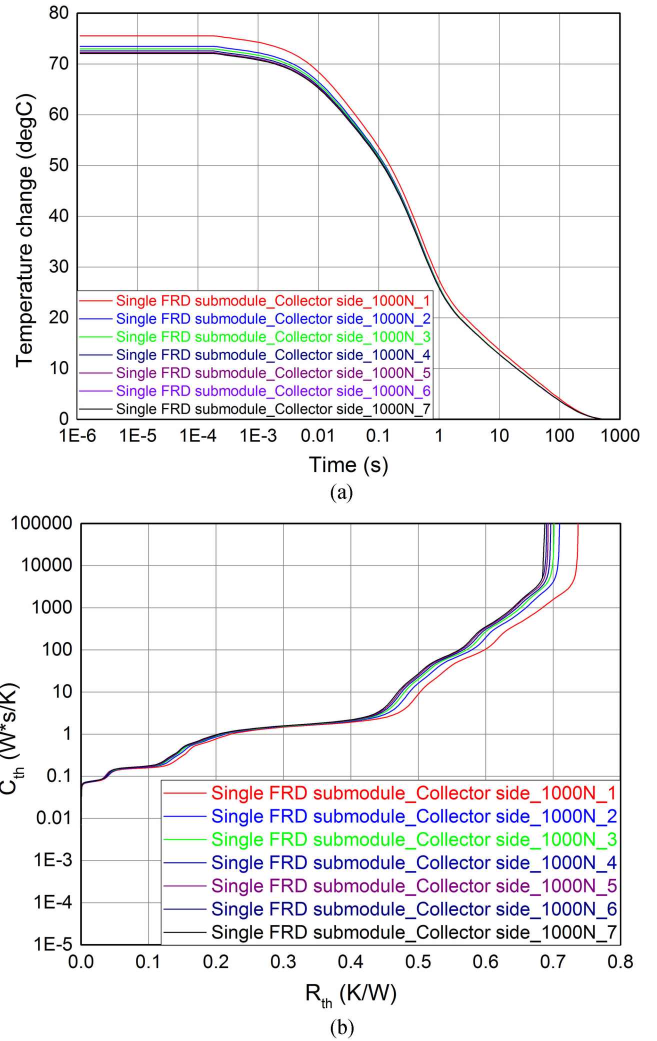

Fig. 8. Experimental results of the single FRD chip submodule with seven times repeatedly measurements. (a) Cooling phase curves. (b) Cumulative structures.

1) Influence of the Temperature: The microhardness of a microcontact will lessen (i.e., it will soften) with the temperature variation of the FRD chip and other components during the measurement, leading to a microcontact elastic deformation, and even plastic deformation under such a high clamping force. Although the temperature is reduced after measurement, the deformation of the microcontact still exists because of the external clamping force, resulting in reduced surface roughness. Thermal contact resistance is reduced as surface roughness decreases, leading to reduced thermal resistance of the submodule.

The single FRD chip submodule cooling curves of the cathode-side cooling under the rated clamping force (@1 kN) are repeatedly measured, and the cumulative structure function is shown in Fig. 8(a) and (b). Numbers 1–7 denote the repeated

TABLE I
THERMAL CONTACT RESISTANCE COMPARISON (K/W)

FEM	Indirectly experiment	This paper
0.0262	0.03	0.026

measurements; external conditions are the same during each measurement.

From the data in Fig. 8(a), it can be seen that the junction temperature of the FRD chip gradually decreases with repeated tests, but the rate of decrease declines slightly. This is because the thermal contact resistance decreases with the deformation of the microcontact during the repeated tests [14]. The results in Fig. 8(b) also show that the bulk thermal resistance of the FRD chip, molybdenum, and cathode pole stays the same with incremental tests. The thermal contact resistance of these two contact interfaces decreases with the increase in the number of measurements, thus leading to a decrease of the submodule's thermal resistance. The data from Fig. 8(b) show that a decrease of two interfaces about 0.026 and 0.015 K/W can be obtained between the first test (#1) and final test (#7), respectively.

The decrement of thermal contact resistance between the silicon chip and cathode-side molybdenum plate is compared with the finite element method (FEM) value and indirectly experimental value from [14]. As shown in Table I, the value obtained through the thermal structure function method proposed in this paper agrees well with the FEM and experimental value.

It can be seen that the components of the submodule are contacted well after several times measurement because the surface roughness will not change. Thus, the changing trend of the thermal contact resistance with high temperature is useful for the real application and other press pack packaging devices. We should measure several times to get the stable one as the final value when the thermal characteristic of power semiconductor is needed to be measured, for example, the junction to case thermal resistance. And meanwhile, in the real application, we should ensure that all the components are contacted well before the device is used.

2) Influence of the Clamping Force: Meanwhile, the transient thermal impedance curves under various clamping forces (0.5, 1, and 3 kN) are also measured to show the influence of the clamping force on the thermal contact resistance, and the transformed cumulative structure functions are shown in Fig. 9.

As shown in Fig. 9, the cumulative structure functions move to the left as the clamping force increases, i.e., the thermal contact resistance is reduced. Thermal resistance on the left side of the red line kept consistent with the clamping force variation is the FRD chip. The reason is that the overall thermal resistance of the FRD chip is invariant to the clamping force. Similarly, a decrease of two interfaces about 0.0424 and 0.1548 K/W can also be obtained with the clamping force of 0.5 and 3 kN, respectively.

It can be seen that the thermal contact resistance depends on the clamping force to a large extent and that we should ensure the uniformity of the clamping force distribution within PP IGBTs. If one silicon chip has a lower clamping force, then the thermal

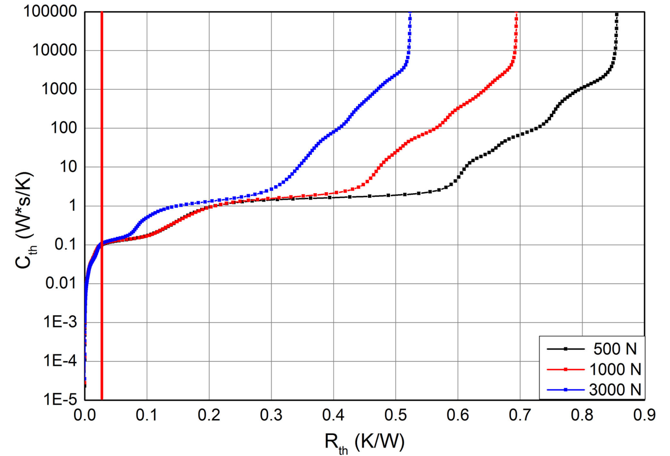

Fig. 9. Cumulative structure of the submodule under various clamping forces.

contact resistance will be higher and finally leads to a higher junction temperature.

From the results regarding the influence of the temperature and clamping force on thermal contact resistance, we have confirmed that the contact interface (thermal contact resistance) corresponds to the area of cumulative structure function with a very small slope. Both the bulk thermal resistance of specific material layers and thermal contact resistance can be clearly identified through the structure functions. The results prove that the method of thermal structure function is accurate enough and is applicable to measure the thermal contact resistance within PP IGBTs.

IV. CONCLUSION

In this paper, the method of thermal structure function is proposed to measure the thermal contact resistance within PP IGBTs. A single FRD chip submodule is fabricated to predict the thermal contact resistance behavior within PP IGBTs through the proposed method. The preliminary conclusions are as follows.

1) Both the bulk thermal resistance of specific material layers and thermal contact resistance between multilayers within PP IGBTs can be identified with thermal structure functions that are derived from a transient thermal impedance curve.
2) All the contact interface thermal contact resistance of the DUT under different working conditions can also be obtained simultaneously through this method. Thus, this thermal contact resistance method is much closer to working conditions, and it is simple to execute.
3) The influence of the temperature and clamping force on thermal contact resistance can be directly reflected via the structure functions, and the resistance change can also be acquired accurately.
4) For PP IGBTs or the press pack packaging style devices, it is important to make all the components contacted well before use and ensure the uniformity of the clamping force distribution among silicon chips.

REFERENCES

[1] F. Wakeman, D. Hemmings, W. Findlay, and G. Lockwood, "Pressure contact IGBT, testing for reliability," Westcode Semicond. Ltd., Wiltshire, U.K., Mar. 2012.

[2] C. Busca, R. Teodorescu, F. Blaabjerg, L. Helle, and T. Abeyasekera, "Dynamic thermal modelling and analysis of press-pack IGBTs both at component-level and chip-level," in *Proc. 39th Annu. Conf. IEEE Ind. Electron. Soc.*, 2013, pp. 677–682.

[3] Z. Ping, Y. Xuan, and L. I. Qiang, "Development on thermal contact resistance," *CIESC J.*, vol. 63, no. 4, pp. 11–20, 2012.

[4] M. Yovanovich and E. Marotta, *Thermal Spreading and Contact Resistances*. Hoboken, NJ, USA: Wiley, 2003, pp. 261–395.

[5] M. A. Lambert and L. S. Fletcher, "Thermal contact conductance of spherical, rough metals," *Trans. ASME Ser. C, J. Heat Transf.*, vol. 119, no. 4, pp. 684–690, 1997.

[6] Y. Z. Li, C. V. Madhusudana, and E. Leonardi, "On the enhancement of the thermal contact conductance: Effect of loading history," *J. Heat Transf.*, vol. 122, no. 1, pp. 46–49, 2000.

[7] T. Mcwaid and E. Marschall, "Thermal contact resistance across pressed metal contacts in a vacuum environment," *Int. J. Heat Mass Transf.*, vol. 35, no. 11, pp. 2911–2920, 1992.

[8] M. Bahrami, "Thermal resistances of gaseous gap for conforming rough contacts" in *Proc. 42nd AIAA Aerosp. Sci. Meeting Exhibit*, 2004, Paper 2004-0821.

[9] *Standard Test Method for Thermal Transmission Properties of Thermally Conductive Electrical Insulation Materials*, ASTM Standard D5470-06, 2006.

[10] Y. Osone, T. Kubo, and N. Nakazato, "Optical measurement of thermal contact conductance between wafer-like thin solid samples," *Trans. ASME Ser. C, J. Heat Transf.*, vol. 121, no. 4, pp. 954–963, 1999.

[11] L. Shi, "Investigation of heat transport on the solid-solid contact interface at low temperature," Huazhong Univ. Sci. Technol., Wuhan, China, 2006.

[12] O. Kwon, L. Shi, and A. Majumdar, "Scanning thermal wave microscopy," *J. Heat Transf.*, vol. 125, pp. 156–163, 2003.

[13] T. Poller *et al.*, "Determination of the thermal and electrical contact resistance in press-pack IGBTs," *Prenatal Diagn.*, vol. 32, no. 13, pp. 1233–1241, 2013.

[14] E. Deng *et al.*, "Optimization of the thermal contact resistance within press pack IGBTs," *Microelectron. Rel.*, vol. 69, pp. 17–28, 2017.

[15] D. L. Blackburn, "Temperature measurements of semiconductor devices - A review," in *Proc. Annu. IEEE Semicond. Therm. Meas. Manage. Symp.*, 2004, vol. 20, pp. 70–80.

[16] L. Yafei, K. Yasushi, and H. Tomoyuki, "Thermal transient test based thermal structure function analysis of IGBT package," in *Proc. Int. Conf. Electron. Packag.*, 2014, pp. 596–599.

[17] U. Scheuermann, "Investigations on the VCE(T)-method to determine the junction temperature by using the chip itself as sensor," in *Proc. Int. Exhib. Conf. Power Electron., Intell. Motion Power Qual.*, Nuremberg, Germany, 2009, pp. 802–807.

[18] *Transient Dual Interface Test Method for the Measurement of the Thermal Resistance Junction-to-Case of Semiconductor Devices With Heat Flow Through a Single Path*, EIA/JEDEC Standard JESD51-14, 2010. [Online]. Available: www.jedec.org

[19] A. Hensler *et al.*, "Thermal impedance spectroscopy of power modules," *Microelectron. Rel.*, vol. 51, no. 51, pp. 1679–1683, 2011.

[20] A. Müsing, G. Ortiz, and J. W. Kolar, "Optimization of the current distribution in press-pack high power IGBT modules," in *Proc. Power Electron. Conf.*, Jun. 2010, pp. 1139–1146.

[21] E. P. Deng *et al.*, "Clamping force distribution within press pack IGBTs," *Trans. China Electrotech. Soc.*, vol. 32, no. 6, pp. 201–208, 2017.

[22] C. Busca, R. Teodorescu, F. Blaabjerg, L. Helle, and T. Abeyasekera, "Dynamic thermal modelling and analysis of press-pack IGBTs both at component-level and chip-level," in *Proc. 39th Annu. Conf. IEEE Ind. Electron. Soc.*, Nov. 2013, pp. 677–682.

[23] T. Poller *et al.*, "Influence of the clamping pressure on the electrical, thermal and mechanical behaviour of press-pack IGBTs," *Microelectron. Rel.*, vol. 53, no. 9, pp. 1755–1759, 2013.

[24] A. A. Hasmasan *et al.*, "Electro-thermo-mechanical analysis of high-power press-pack insulated gate bipolar transistors under various mechanical clamping conditions," *IEEJ J. Ind. Appl.*, vol. 3, no. 3, pp. 192–197, 2014.

[25] E. P. Deng *et al.*, "Clamping force distribution within press pack IGBTs," *Trans. China Electrotech. Soc.*, vol. 32, no. 6, pp. 201–208, 2017.

[26] T. Poller *et al.*, "Mechanical analysis of press-pack IGBTs," *Microelectron. Rel.*, vol. 52, no. 9, pp. 2397–2402, 2012.

[27] A. Hasmasan, C. Busca, R. Teodorescu, and L. Helle, "Modelling the clamping force distribution among chips in press-pack IGBTs using the finite element method," in *Proc. IEEE Int. Symp. Power Electron. Distrib. Gener. Syst.*, 2012, pp. 788–793.

[28] L. Tinschert, A. R. Ardal, T. Poller, M. Bohländer, M. Hernes, and J. Lutz, "Possible failure modes in press-pack IGBTs," *Microelectron. Rel.*, vol. 55, pp. 903–911, 2015.

[29] "Recommendations regarding mechanical clamping of press pack high power semiconductors," ABB, Lenzburg, Switzerland, Appl. Note 5SYA 2036-04, 2016.

[30] "Application note for device mounting instructions," Westcode Semicond. Ltd., Wiltshire, U.K., Mar. 2012.

Authors' photographs and biographies not available at the time of publication.